Published in final edited form as:
Circulation. 2010 May 4; 121(17): 1912–1925. doi:10.1161/CIRCULATIONAHA.109.905471.

CARDIOPROTECTIVE AND ANTI-APOPTOTIC EFFECTS OF HEME OXYGENASE-1 IN THE FAILING HEART

Guangwu Wang, MD, PhD,
Institute of Molecular Cardiology, Department of Medicine, University of Louisville and Louisville VAMC, Louisville, KY

Tariq Hamid, PhD,
Institute of Molecular Cardiology, Department of Medicine, University of Louisville and Louisville VAMC, Louisville, KY

Rachel J. Keith, MS,
Institute of Molecular Cardiology, Department of Medicine, University of Louisville and Louisville VAMC, Louisville, KY

Guihua Zhou, MD, PhD,
Institute of Molecular Cardiology, Department of Medicine, University of Louisville and Louisville VAMC, Louisville, KY

Charles R. Partridge, PhD,
Institute of Molecular Cardiology, Department of Medicine, University of Louisville and Louisville VAMC, Louisville, KY

Xilin Xiang, MD, PhD,
Institute of Molecular Cardiology, Department of Medicine, University of Louisville and Louisville VAMC, Louisville, KY

Justin R. Kingery, BS,
Institute of Molecular Cardiology, Department of Medicine, University of Louisville and Louisville VAMC, Louisville, KY

Robert K. Lewis, MD,
Institute of Molecular Cardiology, Department of Medicine, University of Louisville and Louisville VAMC, Louisville, KY

Qianhong Li, MD, PhD,
Institute of Molecular Cardiology, Department of Medicine, University of Louisville and Louisville VAMC, Louisville, KY

D. Gregg Rokosh, PhD,
Institute of Molecular Cardiology, Department of Medicine, University of Louisville and Louisville VAMC, Louisville, KY

Correspondence: Sumanth D. Prabhu, MD, Division of Cardiovascular Medicine, University of Louisville, ACB, 3rd Floor, 550 South Jackson Street, Louisville, KY 40202, Telephone: (502) 852-7959, Fax: (502) 852-7147, sprabhu@louisville.edu.

DISCLOSURES

There are no commercial affiliations or conflicts of interest to disclose.

Journal Subject Codes: [148] Heart failure - basic studies, [115] Remodeling, [131] Apoptosis

Rachael Ford, BS,
Department of Surgery, Medical University of South Carolina, Charleston, SC

Francis G. Spinale, MD, PhD,
Department of Surgery, Medical University of South Carolina, Charleston, SC

Daniel W. Riggs, BS,
Institute of Molecular Cardiology, Department of Medicine, University of Louisville and Louisville VAMC, Louisville, KY

Sanjay Srivastava, PhD,
Institute of Molecular Cardiology, Department of Medicine, University of Louisville and Louisville VAMC, Louisville, KY

Aruni Bhatnagar, PhD,
Institute of Molecular Cardiology, Department of Medicine, University of Louisville and Louisville VAMC, Louisville, KY

Roberto Bolli, MD, and
Institute of Molecular Cardiology, Department of Medicine, University of Louisville and Louisville VAMC, Louisville, KY

Sumanth D. Prabhu, MD
Institute of Molecular Cardiology, Department of Medicine, University of Louisville and Louisville VAMC, Louisville, KY

Abstract

Background—Heme oxygenase-1 (HO-1) is an inducible stress-response protein that imparts antioxidant and anti-apoptotic effects. However, its pathophysiological role in cardiac remodeling and chronic heart failure (HF) is unknown. We hypothesized that induction of HO-1 in HF ameliorates pathological remodeling.

Methods and Results—Adult male non-transgenic (NTG) and myocyte-restricted HO-1 transgenic (TG) mice underwent either sham operation or coronary ligation to induce HF. Four weeks after ligation, NTG HF mice exhibited post-infarction LV remodeling and dysfunction, hypertrophy, fibrosis, oxidative stress, apoptosis, and reduced capillary density, associated with a two-fold increase in HO-1 expression in noninfarcted myocardium. Compared with NTG, HO-1 TG HF mice exhibited significantly ($p < 0.05$) improved post-infarction survival (94% vs. 57%), and less LV dilatation (end-diastolic volume 46 ± 8 vs. 85 ± 32 μL), mechanical dysfunction (ejection fraction 65 ± 9 vs. 49 ± 16 %), hypertrophy (LV/tibia length 4.4 ± 0.4 vs. 5.2 ± 0.6 mg/mm), interstitial fibrosis (11.2 ± 3.1 vs. 18.5 ± 3.5 %), and oxidative stress (3-fold reduction in tissue malondialdehyde). Moreover, myocyte-specific HO-1 overexpression in HF promoted tissue neovascularization and ameliorated myocardial p53 expression (2-fold reduction) and apoptosis. Inisolated mitochondria, mitochondrial permeability transition (MPT) was inhibited by HO-1 in a carbon monoxide (CO)-dependent manner, and was recapitulated by the CO donor CORM-3. HO-1-derived CO also prevented H_2O_2-induced cardiomyocyte apoptosis and cell death. Finally, in vivo treatment with CORM-3 alleviated post-infarction LV remodeling, p53 expression, and apoptosis.

Conclusions—HO-1 induction in the failing heart is an important cardioprotective adaptation that opposes pathological LV remodeling, and this effect is mediated, at least in part, by CO-dependent inhibition of MPT and apoptosis. Augmentation of HO-1 or its product, CO, may represent a novel therapeutic strategy for ameliorating HF.

Keywords

heme oxygenase-1; heart failure; ventricular remodeling; apoptosis; mitochondrial permeability transition; carbon monoxide

INTRODUCTION

Heme oxygenase-1 (HO-1) is a rapidly inducible cytoprotective protein that degrades heme to biliverdin, ferrous iron, and carbon monoxide (CO) [1]. HO-1 mitigates cellular injury by exerting antioxidant, anti-apoptotic, and anti-inflammatory effects [1–4]; these benefits of HO-1 have been widely demonstrated in a variety of pathological states including hypoxic lung disease [5], vascular injury [6], and cardiac transplant rejection [7]. Conversely, mice with germ-line HO-1 disruption exhibit progressive anemia, inflammation, and oxidative stress with age [8,9]. HO-1-mediated cytoprotection likely reflects the effects of its catalytic products, especially CO, as CO recapitulates the cytoprotective profile of HO-1 and can rescue the injurious effects of HO-1 deficiency [1–4,7,10].

Acute HO-1-mediated cytoprotection extends to the heart. Heterozygous HO-$1^{+/-}$ mice exhibit exaggerated cardiac injury and dysfunction following ischemia/reperfusion (I/R), findings partially rescued by antioxidants [11]. In contrast, mice with cardiac-restricted HO-1 overexpression are resistant to I/R injury, with improved contractile recovery and reduced infarct size, inflammatory cell infiltration, oxidative damage, and apoptosis [12]. Similar results were obtained in rat hearts subjected to I/R 8 weeks after human HO-1 gene transfer [13]; the improvement in left ventricular (LV) function was maintained for up to one year after injury [14]. Nevertheless, even though the salutary effects of HO-1 during short-term cardiac ischemic stress have been established, it is not known whether such a paradigm can be extended to chronic heart failure (HF). This issue is particularly important because HF is characterized by prolonged activation of several stress-response systems (*e.g.*, inflammatory cytokines, catecholamines) that, while initially compensatory and protective, ultimately produce long-term detrimental effects. Although prior studies have reported that HO-1 is upregulated in human failing hearts [15] and in animal models of right ventricular failure [16], it is not clear whether such long-term induction is beneficial or detrimental. Accordingly, in this study we tested the hypothesis that HO-1 upregulation in the failing heart is a cardioprotective adaptation that ameliorates pathological LV remodeling.

MATERIALS AND METHODS

An expanded methods section is included in the accompanying supplement. All studies were performed in compliance with the NIH Guide for the Care and Use of Laboratory Animals (DHHS publication No. [NIH] 85-23, revised 1996).

Mouse models

Male mice (10–16 weeks of age, weighing 25–30 g) were used. Cardiac-specific HO-1 transgenic (TG) mice were obtained from Dr. Shaw-Fang Yet (Harvard Medical School). The HO-1 TG mouse line used expresses 4 copies of a human HO-1 transgene under the control of the α-MyHC promoter [12]. HO-1 TG mice were backcrossed for a minimum of 7 generations into C57BL/6. NTG littermates were used as controls. For *in vivo* CORM-3 supplementation studies, C57BL/6 mice were used.

Coronary ligation

Permanent coronary ligation (or sham operation) in mice was performed as previously described [17]. The mice were followed for 4 weeks after operation.

Echocardiography

Mouse echocardiography was performed and analyzed at baseline and 4 weeks post-operatively as previously described [17].

LV pressure measurement

In a subset of animals, LV mechanical performance was assessed using a Millar pressure-conductance catheter 4 weeks after coronary ligation or sham operation as previously described [18].

Isolation of mouse cardiomyocytes

Ca^{2+}-tolerant mouse ventricular myocytes were isolated using collagenase digestion as previously described [18]. Myocyte cell death was determined using the MTT assay after incubation of isolated myocytes with 500 μM H_2O_2 for 1 h. Absorbance at 550 nm was used to index cell viability. In some studies, myocytes were also exposed to either 50 μM hemoglobin (Hgb, CO scavenger) or 100 μM desferoxamine (DFO, iron chelator) beginning 30 minutes before adding H_2O_2.

H9c2 cardiomyocytes and HO-1 transfection

H9c2 cells (rat embryonic cardiomyoblasts) were obtained from ATCC. Ad5/HO-1, the replication-deficient adenoviral vector containing the entire coding region of rat HO-1 cDNA, was generated in 293 cells by homologous recombination of pCMV/HO-1 and pJM17, a circularized adenovirus genome lacking its E1 region and a portion of the E3 region. Plaque-isolated viral clones were propagated in 293 cells and then purified over two CsCl gradients and titered by plaque assay as previously described [19]. Ad5/LacZ containing the β-galactosidase gene driven by CMV promoter was used as a control vector. H9c2 cells were seeded in 100 mm tissue culture dishes and transiently transfected with Ad5/HO-1 or Ad5/LacZ for 45 min at an MOI of 10 for 72 h prior to treatments.

Immunohistology

Masson Trichrome staining for collagen was performed as previously described [17]. Myocyte cross-sectional area was determined in sections stained with rhodamine-conjugated wheat germ agglutinin (Molecular Probes). Oxidative stress was indexed by immunostaining for malondialdehyde (MDA)-adducted proteins as previously described [20]. For HO-1 immunofluorescent staining, we used anti-mouse HO-1 antibody (Stressgen) and TRITC-conjugated secondary antibody. Immunostaining with FITC-conjugated isolectin B4 (Vector Labs) was performed to determine tissue capillary density. Apoptosis in tissue and cells was determined using the DeadEnd Fluorometric TUNEL System (Promega). Optical sections were obtained with a Zeiss LSM510 inverted confocal scanning laser microscope equipped with Enterprise/argon/HeNe lasers and excitation wavelengths appropriate for multi-channel scanning. For immunohistological analyses, we typically analyzed 6 fields/heart with an area of 66 mm^2/field (total area 396 mm^2/heart).

HO-1 gene expression

Total RNA was isolated from cardiac tissue as previously described [17,20]. HO-1 mRNA was quantified and normalized to mouse beta-actin mRNA using real-time PCR with LUX gene-specific primers (Invitrogen).

Western immunoblotting

Protein extraction, Western immunoblotting, and densitometry were performed as previously described [17,18,20]. Primary antibodies used included anti-p53, anti-poly-ADP ribose polymerase (PARP), anti-Bax, anti-Bcl-2, anti-β-actin, and anti-α-tubulin from Santa Cruz Biotechnology, and anti-HO-1 from StressGen.

Measurement of free MDA by gas chromatography-negative ionization chemical ionization-mass spectrometry (GC-NICI-MS)

Tissue MDA concentration was measured by GC-NICI-MS as previously described [21]. Heart tissue homogenate was derivatized with pentfluorobenzylhydroxylamine (PFBHA) and the PFB-oxime derivatives of MDA were measured by GC-NICI-MS using select ion monitoring mode. Benzaldehyde ring d_5 was used as the internal standard. The following ions were monitored for the indicated aldehyde: benzaldehyde d_5 - m/z 286 (M^+-HF) and MDA m/z 204 (M+-$C_7H_2F_5$-HFNO-C_2H_3).

Mitochondrial membrane permeability transition (MPT)

In adult cardiomyocytes and H9c2 cells, changes in mitochondrial membrane potential ($\Delta\psi_m$) were assessed with tetramethylrhodamine methyl ester (TMRM). TMRM fluorescence was measured at 5-minute intervals for 30 minutes in live cells using a 585-nm long pass filter and laser-scanning confocal microscopy. TMRM is a cationic dye that accumulates in mitochondria in proportion to $\Delta\psi_m$. The TMRM concentration chosen (100 nM) does not suppress mitochondrial respiration [22] and is non-quenching so that mitochondrial depolarization is accompanied by a decrease in cellular TMRM fluorescence over time followed by cell shortening due to ATP depletion [23].The time required for a 2-fold decrease in TMRM fluorescence was taken as an endpoint for MPT.

Mitochondrial MPT pore opening

Mitochondria were isolated from adult mouse hearts and MPT pore (MPTP) opening in isolated mitochondria was induced by Ca^{2+} as previously described [24]. Isolated mitochondria were resuspended in swelling buffer (containing in mmol/L: 120 KCl, 10 Tris·HCl (pH 7.4), 20 MOPS, and 5 KH_2PO_4) to a final protein concentration of 0.25 mg/ml. Mitochondrial swelling induced by pore opening was measured spectrophotometrically as a reduction in absorbance at 520 nm (A_{520}).

Mitochondrial respiration

Mitochondria were resuspended in respiration buffer (pH 7.2) containing in mM: 225 mannitol, 70 sucrose, 10 KH_2PO_4, 1 EGTA. A Clark electrode was used to measure the oxygen content of the mitochondrial suspension with 10 mM pyruvate and 5 mM malate. State 4 respiration was measured at baseline. 330μM ADP was added to stimulate state 3 respiration. The respiratory control ratio (RCR) was defined as the state 3:state 4 respiration ratio. The ADP:O ratio was calculated using total oxygen consumption during state 3 respiration.

Preparation of the CO-donor tricarbonylchloro(glycinato)ruthenium(II) (CORM-3)

CORM-3, a water-soluble transition metal carbonyl drug that stably releases CO, was synthesized following a published protocol [25], and its structure confirmed by infrared spectroscopy and NMR. The synthesized drug was stored at −20°C and fresh solution was made just before use. For control experiments, CORM-3 was inactivated by dissolving it in Krebs-Henseleit buffer and allowing CO liberation overnight at RT.

Statistical analysis

Several statistical techniques were employed. For two-group comparisons, we used the unpaired two sample t test. For comparisons of more than two groups, we used one-way ANOVA if there was one independent variable, two-way ANOVA if there were two independent variables (*e.g.*, genotype and ligation status), and two-way repeated measures ANOVA for matched observations over time with two independent variables. To adjust for multiple comparisons, we performed Student-Newman-Keuls post-test for one-way ANOVA and Bonferroni post-test for two-way ANOVA. Pair-wise comparisons were made between sham groups across genotypes, sham versus HF within each genotype, and HF groups across genotypes. Animal survival was evaluated by the Kaplan-Meier method, and the log-rank test was used to compare survival curves between NTG sham and HF, HO-1 TG sham and HF, and NTG and HO-1 TG HF. A p value of < 0.05 was considered significant. Continuous data are summarized as mean ± SD.

RESULTS

HO-1 is upregulated in murine post-infarction HF

Ten-week old C57BL/6 mice were evaluated 4 weeks after coronary ligation or sham operation. Supplemental Figure 1A shows short-axis LV sections from a sham and failing heart, and M-mode echocardiograms from a mouse at baseline and 4 weeks after myocardial infarction (MI). In this example, a large infarct is present along the anterior and lateral aspects of the LV. Echocardiography revealed marked chamber remodeling with increased LV dimensions and reduced fractional shortening. As shown in Supplemental Figure 1B, there was a 2-fold increase in cardiac HO-1 mRNA and protein levels in HF over sham, without changes in HO-2. HO-1 immunofluorescent staining from WT sham and HF hearts also indicated increased myocyte HO-1 expression in HF as compared to sham (Supplemental Figure 1C). For comparison, staining from NTG and HO-1 TG hearts is also shown, indicating robust HO-1 expression in myocytes but not in the large vessels in HO-1 TG hearts.

HO-1 overexpression improves post-infarction survival and LV remodeling

Baseline echocardiography confirmed the absence of a cardiac phenotype in HO-1 TG mice (Supplemental Table 1). Kaplan-Meier survival curves after coronary ligation or sham operation in NTG and HO-1 TG mice (Figure 1A) revealed that whereas mortality in NTG HF was markedly higher than NTG sham, myocyte-specific HO-1 overexpression imparted a survival benefit at 28 days post-infarction. Figures 1B–1C show short-axis LV sections, M-mode echocardiograms, and group data from NTG and HO-1 TG sham and failing hearts. There was significant chamber dilatation (increased LVEDV and LVESV) and systolic dysfunction (reduced LVEF) in both HF groups over sham. However, in comparison with NTG HF, LV dilatation and dysfunction were attenuated in HO-1 TG HF. Indeed, in the example in Figure 1B, this occurred despite larger overall infarct size in the HO-1 TG mouse. The LV/tibia length ratio showed a similar response pattern (Figure 1D), indicating less hypertrophy in HO-1 TG HF. Hemodynamic recordings (Figure 1F) and pressure-volume loops (Figure 1G) indicated improved contractility, LV dilatation, LV filling pressure, and diastolic function in HO-1 TG HF as compared to NTG HF, without appreciable differences between sham groups (Table). Notably, overall group infarct size was similar in NTG and HO-1 TG HF (Figure 1E), suggesting that differences in remodeling and survival were independent of the degree of initial injury. Collectively the data show that HO-1 overexpression alleviates post-infarction LV remodeling and improves mechanical performance.

HO-1 overexpression attenuates hypertrophy, fibrosis, and oxidant stress in the failing heart

Cell membrane staining with rhodamine wheat germ agglutinin revealed myofiber hypertrophy in both NTG and HO-1 TG HF when compared with sham-operated hearts (Figure 2A). The degree of hypertrophy, however, was attenuated in HO-1 TG HF hearts, confirming the gravimetric data (Figure 1D). To evaluate myocardial oxidative stress, we evaluated both protein-bound MDA by immunostaining and free MDA by GC-NICI-MS. As seen by the immunostains in Figure 2B, MDA-modified proteins were increased in both HF groups over sham but significantly less so in HO-1 TG HF. Figure 2C shows representative GC-chromatograms (Left), the m/z values of ions 286 (benzaldehyde d5) and 204 (MDA) (Center), and the GC-NICI-MS quantitative group data (Right). HF in NTG mice increased tissue MDA levels 2-fold over NTG sham. In contrast, myocyte-specific HO-1 overexpression completely prevented the HF-associated increase in tissue MDA. These data indicate a potent anti-oxidant effect of HO-1 in the remodeling heart. Additionally, Masson's trichrome staining (Figure 2D) revealed less collagen deposition in the remote myocardium of HO-1 TG HF hearts, suggesting an anti-fibrotic effect of HO-1.

HO-1 is anti-apoptotic and promotes neovascularization in the failing heart

Figure 3A shows representative TUNEL stains (with Troponin I co-staining) from the remote and border zone of a NTG HF heart, illustrating TUNEL positive nuclei. Quantitative data demonstrated that NTG and HO-1 TG HF groups exhibited significantly greater apoptosis of both myocytes and non-myocytes (differentiated on the basis of attendant troponin I co-staining) than their respective sham. The apoptotic rate we observed in the failing heart (~0.50%) was both consistent with that reported for human HF (~0.12 – 0.70%) [26], and physiologically significant as sustained apoptotic rates as low as 0.23% induce dilated cardiomyopathy in mice [27]. However, HO-1 TG HF hearts exhibited a significant reduction in myocyte and non-myocyte apoptotic rate vs. NTG HF. As a second measure of apoptosis, we determined myocardial levels of cleaved and uncleaved PARP protein. As seen in Figure 3B, the ratio of cleaved:uncleaved PARP increased in NTG HF over sham (indicating enhanced apoptosis), but did not change appreciably between HO-1 TG sham and HO-1 TG HF, consistent with the TUNEL stains. Moreover, the protein level of p53, a central transcriptional activator of multiple pro-apoptotic genes, was increased two-fold in NTG HF. This increase was suppressed in HO-1 TG HF (with p53 levels ~50% lower than in NTG mice) as well as in HO-1 TG sham hearts (Figure 3B). As p53 also has prominent anti-angiogenic effects [28], we also determined the effects of cardiac HO-1 overexpression on tissue neovascularization post-infarction. As shown in Figure 3C, isolectin staining revealed that LV capillary density (excluding LV scar) was markedly decreased in NTG HF in comparison with sham-operated hearts, but was maintained in HO-1 TG HF. Moreover, among the HF groups, border zone capillary density was also significantly higher in HO-1 TG hearts. These results establish that HO-1 exerts important anti-apoptotic effects and promotes neovascularization in the failing heart, potentially related in part to p53.

HO-1 suppresses mitochondrial respiration, MPT, and cardiomyocyte apoptosis in a CO-dependent manner

We next evaluated the effects of HO-1 on mitochondrial respiration, MPT, and cardiomyocyte apoptosis. In HO-1 TG hearts, robust levels of HO-1 were associated with the mitochondrial fraction (~40% of total) indicating physical proximity of HO-1 to the mitochondrial pore in these hearts but not in WT hearts (Figure 4A). Respiration studies were performed in freshly isolated mitochondria from NTG and HO-1 TG hearts in the presence or absence of the CO donor CORM-3 (iCORM-3 control) or the CO scavenger hemoglobin. ADP:O ratios were similar among all experimental groups, ranging from 2.1 ±

0.05 to 2.8 ± 0.22, indicating a relatively constant relationship between ATP synthesis and oxygen consumption (data not shown). In contrast, the ratio of state 3:state 4 respiration (RCR) was suppressed in both HO-1 TG mitochondria as well as NTG mitochondria incubated with CORM-3 but not inactive iCORM-3 (Figure 4B). Both HO-1 TG mitochondria and NTG mitochondria treated with CORM-3 showed a general increase in absolute state 3 and state 4 respiration (Supplemental Figure 2), although overall, respiration was suppressed. The increase in CO did not change coupling as the ADP:O ratio was not affected (data not shown). Moreover, the suppressed state 3:state 4 ratio in HO-1 TG mitochondria was normalized upon incubation with the CO scavenger hemoglobin, indicating CO-dependence of this effect. Ca^{2+}-induced mitochondrial swelling assays were then performed to assess MPT (Figure 4C). Robust swelling was induced by Ca^{2+} in NTG cardiac mitochondria; this was prevented by the MPT pore inhibitor cyclosporine A (CsA) as well as by CORM-3 (but not iCORM-3). HO-1 TG cardiac mitochondria were resistant to swelling, a response that was reversed by co-incubation with hemoglobin. NTG mitochondria pretreated with recombinant HO-1 protein were also less susceptible to Ca^{2+}-induced MPT (Supplemental Figure 3).

We next measured $\Delta\psi_m$ and MPT in living adult cardiomyocytes or H9c2 cells. WT or HO-1 TG cardiomyocytes were loaded with TMRM, and phenylarsine oxide (PAO, 20 μM) was used to induce MPT. The time required for a 2-fold decrease in TMRM fluorescence was taken as an endpoint for MPT. TMRM mitochondrial labeling revealed the typical cardiomyocyte pattern of fluorescent bands oriented along the longitudinal axis of adult cardiomyocytes or a striking punctuate pattern in H9c2 cells (Supplemental Figure 4). In WT cardiomyocytes, PAO induced MPT within 15 min, as indicated by the decline in TMRM fluorescence (Figure 5A). The fluorescence decline was largely prevented by CsA, showing that the change was specifically a consequence of MPT. In comparison to WT myocytes, MPT induction was significantly delayed in HO-1 TG cardiomyocytes, analogous to the results of the mitochondrial swelling studies. Moreover, pretreatment of H9c2 cardiomyocytes with CORM-3, but not iCORM-3, attenuated PAO-induced MPT (Supplemental Figure 5), and H9c2 cells transfected with HO-1 adenovirus, which augmented HO-1 co-localization with mitochondria (Supplemental Figure 6), were more resistant to H_2O_2-induced MPT, as indexed by TMRM labeling (Supplemental Figure 7). Taken together, these results suggest that HO-1, in large part via CO, inhibits both mitochondrial respiration and MPT in cardiomyocytes.

We further evaluated whether the products of HO-1 catalysis had analogous protective effects on cardiomyocyte apoptosis and cell death. H_2O_2-induced apoptosis was evaluated by TUNEL staining and cell death by MTT assay. H_2O_2 (100 μM) induced robust apoptosis (Figure 5B) and cell death (Figure 5C) in WT myocytes but not in HO-1 TG myocytes. The resistance of HO-1 TG myocytes to H_2O_2-induced cell death was abrogated upon co-treatment with hemoglobin and, to a lesser extent, with the iron chelator desferoxamine (DFO). However, the interpretation of the latter was confounded by the finding that DFO alone also induced cell death (albeit to a lesser degree) in both WT and HO-1 TG myocytes. Taken together, analogous to its effect on MPT, HO-1 is anti-apoptotic in cardiomyocytes, an effect in large part a consequence of its product CO (and perhaps ferrous iron). Collectively, these data suggest that CO-mediated prevention of MPT may be one important mechanism underlying the anti-apoptotic effects of HO-1 in HF.

CORM-3 treatment in vivo alleviates post-infarction LV remodeling

Having found that CO is a key cytoprotective mediator of the anti-apoptotic effects of HO-1, we tested whether CORM-3 treatment would attenuate LV remodeling after MI in vivo. C57BL/6 mice were subjected to coronary ligation and, starting 4 days later, were administered 40 mg/kg CORM-3 i.p. daily for 24 days, after which LV remodeling and

function were assessed using echocardiography and tissue morphometry. The biologic activity of this dose of CORM-3 was tested by measuring blood carboxyhemoglobin (COHb). Prior to drug administration, COHb in the blood was ~1%, whereas 2–6 h after injection, COHb increased to 5.9 ± 0.6% and remained at this level for 24 h, indicating long-lasting systemic delivery of CO. Figure 6A shows representative LV sections from a sham animal, a HF animal without CORM-3, and a HF animal with CORM-3 treatment. In comparison with untreated HF, the CORM-3 treated heart had less LV dilatation and remodeling. Group echocardiographic and gravimetric data 4 weeks after infarction revealed that chronic CORM-3 administration attenuated LV dilatation, improved systolic function and reduced LV hypertrophy despite equivalent infarct size between untreated and treated groups (Figure 6B–6C). Hemodynamic data also indicated better LV mechanical performance with CORM-3, with improvements in dP/dt_{max}/IP, tau, and LVEDP over untreated HF. The CORM-3-mediated benefits occurred despite equivalent afterload in the treated and untreated groups (LV peak systolic pressure 84 ± 4 vs. 84 ± 10 mm Hg, untreated vs. CORM-3 treated HF, p = NS) (Figure 6D). Moreover, as was the case with HO-1 TG mice, infarcted mice treated with CORM-3 also exhibited markedly reduced p53 expression (Figure 6E) and less myocardial apoptosis by TUNEL staining (Figure 6F) than untreated HF mice. Figure 6G depicts expression of Bax, a pro-apoptotic protein that can be induced by p53, and Bcl-2, an anti-apoptotic protein that can be repressed by p53 [29]. Compared to untreated HF, CORM-3 HF hearts exhibited significantly augmented Bcl-2 levels and a trend (although not statistically significant) toward reduced Bax expression. These results are consistent with a p53-mediated effect in CORM-3 treated HF hearts, and are also in line with the observed reduction in apoptotic rate. These data demonstrate that exogenous CO administration by CORM-3 alleviates post-infarction LV remodeling and apoptosis, and that in the failing heart, exogenous CO augments the cardioprotective effects of HO-1 upregulation.

DISCUSSION

In this study we show for the first time that HO-1 induction in the failing heart is a cardioprotective adaptation that alleviates post-infarction pathological LV remodeling, an effect mediated in part by CO-dependent anti-apoptotic actions that are associated with, and likely due to, prevention of MPT. Several lines of evidence support these conclusions. First, HO-1 expression was upregulated two-fold in chronically remodeled failing myocardium remote from the infarct, and well after the formation of a stable scar. Second, HO-1 overexpression and gain-of-function in the heart ameliorated LV dilatation and dysfunction, hypertrophy, interstitial fibrosis, and oxidative stress, and improved tissue neovascularization. These results indicate both a cardioprotective (anti-hypertrophic, antioxidant, anti-fibrotic, and pro-angiogenic) role of HO-1 in HF and a potential therapeutic effect of enhancing HO-1 function over and above the two-fold upregulation seen in HF. Third, our observations in HO-1 TG mice establish an *in vivo* anti-apoptotic effect of HO-1 in the failing heart that mitigates cell loss, p53 expression, and pathological remodeling. Fourth, in isolated mitochondria and cardiomyocytes, we found that HO-1, primarily via CO, suppresses the mitochondrial RCR and MPT, and inhibits apoptosis. Lastly, sustained CO donor treatment *in vivo* alleviated post-infarction remodeling and attenuated apoptosis in a manner similar to HO-1 overexpression, further underscoring the potential utility of enhancing the HO-1 axis in chronic HF. Taken together, these findings indicate that augmentation of HO-1 and/or its product, CO, may represent novel and beneficial therapeutic approaches in HF.

HO-1 upregulation is a cardioprotective adaptation in the failing heart

The cytoprotective effects of HO-1 are mediated by its product CO (which is generated exclusively by the HO system), the production of the antioxidants biliverdin and bilirubin, and the degradation of excess amounts of the pro-oxidant heme [1,2]. Previous studies have shown cardioprotective actions of HO-1 in models of acute stress (e.g., ischemia/reperfusion injury) [11–14]. However, the role of HO-1 in chronic cardiac remodeling and HF is virtually unknown. Although prior studies have reported HO-1 upregulation in remodeled myocardium resulting from mechanical overload and neurohormonal stimulation [15,16], as well as in experimental and human HF [15,30], its significance is poorly understood. Specifically, no information is available regarding whether HO-1 is an important modulator of pathological remodeling and, if so, which mechanisms underlie such an effect. These questions are particularly important because chronic upregulation of a compensatory system may not necessarily induce the same effects seen during the acute stress-response (for example pro-inflammatory cytokines are acutely protective but detrimental over the long-term); hence, the short-term actions of HO-1 cannot necessarily be extrapolated to a chronic setting. Moreover, the same catalytic products that are responsible for HO-1-mediated acute cardioprotection (bilirubin, free iron, or CO) can potentially induce toxicity at inordinately high (or inappropriately sustained) levels [1].

Our results establish that the upregulation of HO-1 in the failing heart ameliorates detrimental remodeling. Using genetically-engineered mice, we found that sustained HO-1 expression in failing myocardium promotes neovascularization and limits oxidative stress, myofiber hypertrophy, interstitial fibrosis, and apoptosis and p53 expression. These responses were associated with improved chamber remodeling, and systolic and diastolic function. The central importance of HO-1 in HF is highlighted by its ability to favorably modulate oxidative stress, neovascularization, and apoptosis, three key events that are known to independently influence remodeling. Our studies in HO-1 TG mice suggest that further enhancement of HO-1 activity beyond what is normally achieved in the failing heart may be a novel therapeutic strategy to prevent progression of disease. One important, though not exclusive, mechanism of these beneficial effects appears to be the moderation of apoptosis.

HO-1 modulation of apoptosis and the role of CO

Although HO-1 is known to inhibit apoptosis [1–3], the precise mechanisms by which this occurs remain obscure. Apoptosis in the failing heart involves multiple mechanisms that produce heightened activity of extrinsic death-receptor pathways or intrinsic mitochondrial and/or endoplasmic reticulum-linked pathways [31]. Emerging evidence supports an important role for mitochondria as arbiters of cell fate in the failing heart. Intrinsic pathways converge on the mitochondria to induce mitochondrial remodeling and dysfunction, which in turn leads to the release of apoptogenic proteins such as cytochrome *c* into the cytosol and the activation of terminal caspase cascades [31]. A central event that is thought to trigger mitochondrial dysfunction and cytochrome *c* release is MPT, with subsequent opening of the mitochondrial pore and mitochondrial swelling [31,32]. While in early stages, brief MPT could be protective, prolonged opening of the pore is usually considered detrimental because it triggers both necrosis and apoptosis [32]. Indeed, MPT contributes to the loss of mitochondrial function observed in the failing heart [33], and LV remodeling is associated with an increase in mitochondrial pore opening in hearts both 12 and 18 weeks after coronary ligation [34]. In addition, CsA, a potent blocker of MPT, improves mitochondrial function in failing cardiomyocytes [33].

A key finding of our study is that HO-1 reduces the RCR in cardiac mitochondria and confers increased resistance to prolonged MPT triggered by a variety of inducers including

PAO, calcium-overload, and oxidative stress (H_2O_2), suggesting that reduced respiration:phosphorylation coupling and improved mitochondrial membrane stability in the face of cellular stress may underlie the cardioprotective and anti-apoptotic effects of HO-1 in HF. HO-1 also produced greater resistance to apoptosis and cell death in cardiomyocytes, akin to the *in vivo* findings in HO-1 TG HF. Importantly, the beneficial effects of HO-1 on respiration, MPT, and apoptosis were associated with physical approximation of HO-1 with the mitochondria, and were prevented upon scavenging of CO but recapitulated by CORM-3, indicating that CO plays a primary role in the modulation of mitochondrial function and apoptosis. The *in vivo* observations that cardiac myocyte-restricted overexpression of HO-1 also reduced non-myocyte apoptosis in HO-1 TG HF further supports the notion that a small freely diffusible molecule such as CO mediates these effects. Moreover, our results in cardiomyocytes are consistent with previous studies demonstrating that CO inhibits p53 expression and mitochondrial cytochrome *c* release in vascular smooth muscle cells exposed to pro-inflammatory cytokines [35], suppresses free radical production in activated macrophages [36], and protects PC12 cells from peroxynitrite-induced apoptosis by preventing the depolarization of mitochondrial transmembrane potential [37]. It is possible that HO-1-mediated inhibition of apoptosis may be related to other mechanisms in addition to CO, as iron chelation with DFO also mitigated the anti-apoptotic effect of HO-1 to some degree. Regardless, our observations indicate that CO-dependent inhibition of MPT, attendant mitochondrial remodeling, and apoptosis can contribute to the potent anti-apoptotic effect of HO-1 in the failing heart.

If CO-mediated MPT prevention is primarily responsible for the anti-apoptotic and cardioprotective effect of HO-1 in HF, then bypassing the HO-1 system with pharmacological delivery of CO should achieve similar benefits. Our studies with CORM-3 support this concept, since chronically delivered exogenous CO (CORM-3) recapitulated the effects of HO-1 transgenesis on pathological LV remodeling and dysfunction, apoptosis, and p53 expression. Importantly, the CORM-3-induced remodeling responses occurred without appreciable changes in systolic pressure, indicating a direct effect of CO on the myocardium rather than an indirect effect due to changes in afterload. Many prior studies of CO-mediated effects *in vivo* have used CO inhalation as a means of delivery, an approach that is quantitatively difficult to standardize with regard to dosing and therefore prone to potential toxicity. Moreover, CO inhalation exerts many nonspecific and potentially untoward effects. For these reasons, we used CORM-3, a carrier of CO that releases CO in a predictable and stable manner [25]. The dose that we used chronically increased COHb to ~6%, and was identical to that used by Motterlini and colleagues in a murine cardiac transplant rejection model [25]. Further studies will be required to optimize the dose of CORM-3 for chronic CO delivery to the heart and to comprehensively determine the mechanisms underlying CORM-3-mediated improvements in LV remodeling. Nevertheless, our present findings suggest that pharmacological CO delivery may be of potential therapeutic value in HF and that feasibility of this approach should be explored in the clinical setting.

In summary, the studies reported herein reveal a novel pathophysiological role of HO-1 that was heretofore unrecognized. Our results establish that sustained HO-1 upregulation in the failing heart is an important beneficial adaptation that serves to counteract detrimental LV remodeling via antioxidant, anti-hypertrophic, anti-fibrotic, and pro-angiogenic effects. We have also identified an *in vivo* anti-apoptotic action of HO-1 in the failing heart that mitigates progressive cell loss. Our *in vitro* analyses support the concept that this effect is related, at least in part, to CO-mediated stabilization of mitochondrial pore opening. Consistent with a central role for CO in HO-1-dependent chronic cardioprotection, exogenous CO delivery *in vivo* using CORM-3 also improved post-infarction LV remodeling and dysfunction and reduced myocardial apoptosis. These findings have both conceptual and practical implications. From a conceptual standpoint, they reveal a new facet

of the pathophysiology of HF, that is, the cardioprotective role of HO-1. From a practical standpoint, augmentation of the HO-1 axis and/or ambient CO levels should be explored as therapeutic approaches to limit pathological LV remodeling in HF.

Clinical Impact Commentary

Heme oxygenase-1 (HO-1), which degrades heme to biliverdin, ferrous iron, and carbon monoxide (CO), is rapidly inducible and cardioprotective during acute stress. However, its pathophysiological role in chronic heart failure (HF) is unknown. Using myocyte-restricted HO-1 transgenic (TG) mice, we evaluated whether HO-1 upregulation in the failing heart is a beneficial adaptation that alleviates pathological remodeling. Non-transgenic (NTG) and HO-1 TG mice underwent either sham operation or permanent left coronary ligation to induce HF. After four weeks, as compared with NTG mice with HF, HO-1 TG mice with HF exhibited improved post-infarction survival, and significantly less LV dilatation and dysfunction, cardiac hypertrophy, fibrosis, and oxidative stress, together with improved tissue neovascularization and reduced myocardial p53 expression and apoptosis. In isolated mitochondria, mitochondrial permeability transition (MPT) was inhibited by HO-1 in a CO-dependent manner, and was recapitulated by the CO donor CORM-3. HO-1-derived CO also prevented H_2O_2-induced cardiomyocyte apoptosis and cell death. Lastly, chronic *in vivo* treatment with CORM-3 alleviated post-infarction LV remodeling, p53 expression, and apoptosis in wild-type mice. Our results establish that sustained HO-1 upregulation in HF is an important beneficial adaptation that serves to counteract detrimental LV remodeling via antioxidant, anti-hypertrophic, antifibrotic, and pro-angiogenic effects. We have also identified an in vivo anti-apoptotic action of HO-1 in the failing heart that is related, at least in part, to CO-mediated stabilization of mitochondrial pore opening. Therefore, augmentation of HO-1 or its product, CO, should be explored as therapeutic approaches to limit pathological LV remodeling and myocyte loss in HF.

Supplementary Material

Refer to Web version on PubMed Central for supplementary material.

Acknowledgments

FUNDING SOURCES

This work was supported by National Institute of Health Grants HL-78825, ES-11860, HL-55757, HL-70897, HL-76794, HL-55477, and a VA Merit Award.

REFERENCES

1. Otterbein LE, Choi AM. Heme oxygenase: colors of defense against cellular stress. Am J Physiol Lung Cell Mol Physiol. 2000; 279:L1029–L1037. [PubMed: 11076792]
2. Abraham NG, Kappas A. Heme oxygenase and the cardiovascular–renal system. Free Radic Biol Med. 2005; 39:1–25. [PubMed: 15925276]
3. Brouard S, Otterbein LE, Anrather J, Tobiasch E, Bach FH, Choi AM, Soares MP. Carbon monoxide generated by heme oxygenase 1 suppresses endothelial cell apoptosis. J Exp Med. 2000; 192:1015–1026. [PubMed: 11015442]
4. Lee TS, Chau LY. Heme oxygenase-1 mediates the anti-inflammatory effect of interleukin-10 in mice. Nature Med. 2002; 8:240–246. [PubMed: 11875494]
5. Christou H, Morita T, Hsieh CM, Koike H, Arkonac B, Perrella MA, Kourembanas S. Prevention of hypoxia-induced pulmonary hypertension by enhancement of endogenous heme oxygenase-1 in the rat. Circ Res. 2000; 86:1224–1229. [PubMed: 10864912]

6. Duckers HJ, Boehm M, True AL, Yet SF, San H, Park JL, Clinton Webb R, Lee ME, Nabel GJ, Nabel EG. Heme oxygenase-1 protects against vascular constriction and proliferation. Nature Med. 2001; 7:693–698. [PubMed: 11385506]
7. Sato K, Balla J, Otterbein L, Smith RN, Brouard S, Lin Y, Csizmadia E, Sevigny J, Robson SC, Vercellotti G, Choi AM, Bach FH, Soares MP. Carbon monoxide generated by heme oxygenase-1 suppresses the rejection of mouse-to-rat cardiac transplants. J Immunol. 2001; 166:4185–4194. [PubMed: 11238670]
8. Poss KD, Tonegawa S. Heme oxygenase 1 is required for mammalian iron reutilization. Proc Natl Acad Sci USA. 1997; 94:10919–10924. [PubMed: 9380735]
9. Poss KD, Tonegawa S. Reduced stress defense in heme oxygenase 1-deficient cells. Proc Natl Acad Sci USA. 1997; 94:10925–10930. [PubMed: 9380736]
10. Morita T, Kourembanas S. Endothelial cell expression of vasoconstrictors and growth factors is regulated by smooth muscle cell-derived carbon monoxide. J Clin Invest. 1995; 96:2676–2682. [PubMed: 8675634]
11. Yoshida T, Maulik N, Ho YS, Alam J, Das DK. H(mox-1) constitutes an adaptive response to effect antioxidant cardioprotection: A study with transgenic mice heterozygous for targeted disruption of the heme oxygenase-1 gene. Circulation. 2001; 103:1695–1701. [PubMed: 11273999]
12. Yet SF, Tian R, Layne MD, Wang ZY, Maemura K, Solovyeva M, Ith B, Melo LG, Zhang L, Ingwall JS, Dzau VJ, Lee ME, Perrella MA. Cardiac-specific expression of heme oxygenase-1 protects against ischemia and reperfusion injury in transgenic mice. Circ Res. 2001; 89:168–173. [PubMed: 11463724]
13. Melo LG, Agrawal R, Zhang L, Rezvani M, Mangi AA, Ehsan A, Griese DP, Dell'Acqua G, Mann MJ, Oyama J, Yet SF, Layne MD, Perrella MA, Dzau VJ. Gene therapy strategy for long-term myocardial protection using adeno-associated virus-mediated delivery of heme oxygenase gene. Circulation. 2002; 105:602–607. [PubMed: 11827926]
14. Liu X, Simpson JA, Brunt KR, Ward CA, Hall SR, Kinobe RT, Barrette V, Tse MY, Pang SC, Pachori AS, Dzau VJ, Ogunyankin KO, Melo LG. Preemptive heme oxygenase-1 gene delivery reveals reduced mortality and preservation of left ventricular function 1 yr after acute myocardial infarction. Am J Physiol Heart Circ Physiol. 2007; 293:H48–H59. [PubMed: 17322421]
15. Grabellus F, Schmid C, Levkau B, Breukelmann D, Halloran PF, August C, Takeda N, Takeda A, Wilhelm M, Deng MC, Baba HA. Reduction of hypoxia-inducible heme oxygenase-1 in the myocardium after left ventricular mechanical support. J Pathol. 2002; 197:230–237. [PubMed: 12015748]
16. Raju VS, Imai N, Liang CS. Chamber-specific regulation of heme oxygenase-1 (heat shock protein 32) in right-sided congestive heart failure. J Mol Cell Cardiol. 1999; 31:1581–1589. [PubMed: 10423355]
17. Hamid T, Gu Y, Ortines R, Bhattacharya C, Wang GW, Xuan YT, Prabhu SD. Divergent TNF receptor-related remodeling responses in heart failure: role of NF-κB and inflammatory activation. Circulation. 2009; 119:1386–1397. [PubMed: 19255345]
18. Luo J, Hill BG, Gu Y, Cai J, Srivastava S, Bhatnagar A, Prabhu SD. Mechanisms of acrolein-induced myocardial dysfunction: implications for environmental and endogenous aldehyde exposure. Am J Physiol Heart Circ Physiol. 2007; 293:H3673–H3684. [PubMed: 17921335]
19. Li Q, Guo Y, Tan W, Ou Q, Wu WJ, Sturza D, Dawn B, Hunt G, Cui C, Bolli R. Cardioprotection afforded by inducible nitric oxide synthase gene therapy is mediated by cyclooxygenase-2 via a nuclear factor-κB dependent pathway. Circulation. 2007; 116:1577–1584. [PubMed: 17785622]
20. Srivastava S, Chandrasekar B, Gu Y, Luo J, Hamid T, Hill BG, Prabhu SD. Downregulation of CuZn-superoxide dismutase contributes to β-adrenergic receptor-mediated oxidative stress in the heart. Cardiovasc Res. 2007; 74:445–455. [PubMed: 17362897]
21. Srivastava S, Vladykovskaya E, Barski OA, Spite M, Kaiserova K, Petrash JM, Chung SS, Hunt G, Dawn B, Bhatnagar A. Aldose reductase protects against early atherosclerotic lesion formation in apolipoprotein E-null mice. Circ Res. 2009; 105:793–802. [PubMed: 19729598]
22. Scaduto RC Jr, Grotyohann LW. Measurement of mitochondrial membrane potential using fluorescent rhodamine derivatives. Biophys J. 1999; 76:469–477. [PubMed: 9876159]

23. Levraut J, Iwase H, Shao ZH, Vanden Hoek TL, Schumacker PT. Cell death during ischemia: relationship to mitochondrial depolarization and ROS generation. Am J Physiol Heart Circ Physiol. 2003; 284:H549–H558. [PubMed: 12388276]
24. Wang G, Liem DA, Vondriska TM, Honda HM, Korge P, Pantaleon DM, Qiao X, Wang Y, Weiss JN, Ping P. Nitric oxide donors protect murine myocardium against infarction via modulation of mitochondrial permeability transition. Am J Physiol Heart Circ Physiol. 2005; 288:H1290–H1295. [PubMed: 15528225]
25. Clark JE, Naughton P, Shurey S, Green CJ, Johnson TR, Mann BE, Foresti R, Motterlini R. Cardioprotective actions by a water-soluble carbon monoxide-releasing molecule. Circ Res. 2003; 93:e2–e8. [PubMed: 12842916]
26. van Empel VP, Bertrand AT, Hofstra L, Crijns HJ, Doevendans PA, De Windt LJ. Myocyte apoptosis in heart failure. Cardiovasc Res. 2005; 67:21–29. [PubMed: 15896727]
27. Wencker D, Chandra M, Nguyen K, Miao W, Garantziotis S, Factor SM, Shirani J, Armstrong RC, Kitsis RN. A mechanistic role for cardiac myocyte apoptosis in heart failure. J Clin Invest. 2003; 111:1497–1504. [PubMed: 12750399]
28. Teodoro JG, Evans SK, Green MR. Inhibition of tumor angiogenesis by p53: a new role for the guardian of the genome. J Mol Med. 2007; 85:1175–1186. [PubMed: 17589818]
29. Miyashita T, Krajewski S, Krajewska M, Wang HG, Lin HK, Liebermann DA, Hoffman B, Reed JC. Tumor suppressor p53 is a regulator of bcl-2 and bax gene expression in vitro and in vivo. Oncogene. 1994; 9:1799–1805. [PubMed: 8183579]
30. Lakkisto P, Palojoki E, Backlund T, Saraste A, Tikkanen I, Voipio-Pulkki LM, Pulkki K. Expression of heme oxygenase-1 in response to myocardial infarction in rats. J Mol Cell Cardiol. 2002; 34:1357–1365. [PubMed: 12392996]
31. Foo RS, Mani K, Kitsis RN. Death begets failure in the heart. J Clin Invest. 2005; 115:565–571. [PubMed: 15765138]
32. Baines CP. The mitochondrial permeability transition pore and ischemia-reperfusion injury. Basic Res Cardiol. 2009; 104:181–188. [PubMed: 19242640]
33. Sharov VG, Todor A, Khanal S, Imai M, Sabbah HN. Cyclosporine A attenuates mitochondrial permeability transition and improves mitochondrial respiratory function in cardiomyocytes isolated from dogs with heart failure. J Mol Cell Cardiol. 2007; 42:150–158. [PubMed: 17070837]
34. Javadov S, Huang C, Kirshenbaum L, Karmazyn M. NHE-1 inhibition improves impaired mitochondrial permeability transition and respiratory function during postinfarction remodelling in the rat. J Mol Cell Cardiol. 2005; 38:135–143. [PubMed: 15623430]
35. Liu XM, Chapman GB, Peyton KJ, Schafer AI, Durante W. Carbon monoxide inhibits apoptosis in vascular smooth muscle cells. Cardiovasc Res. 2002; 55:396–405. [PubMed: 12123779]
36. Srisook K, Han SS, Choi HS, Li MH, Ueda H, Kim C, Cha YN. CO from enhanced HO activity or from CORM-2 inhibits both O2- and NO production and downregulates HO-1 expression in LPS-stimulated macrophages. Biochem Pharmacol. 2006; 71:307–318. [PubMed: 16329999]
37. Li MH, Cha YN, Surh YJ. Carbon monoxide protects PC12 cells from peroxynitrite-induced apoptotic death by preventing the depolarization of mitochondrial transmembrane potential. Biochem Biophys Res Commun. 2006; 342:984–990. [PubMed: 16598857]

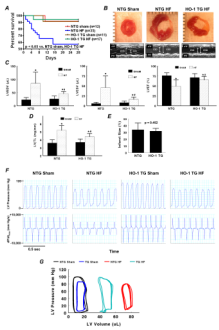

Figure 1.

Transgenic expression of HO-1 improves post-infarction LV remodeling. ***A***, Kaplan-Meier curves after coronary ligation or sham operation in NTG and HO-1 TG mice. HF, heart failure. ***B*** and ***C***, short-axis LV sections and M-mode echocardiograms, and group echocardiographic data from NTG and HO-1 TG sham and HF hearts. ***D***, LV/tibia length (TL) ratio from NTG and HO-1 TG sham and HF hearts. ***E***, Mean infarct size in NTG and HO-1 TG HF hearts. NS, not significant. ***F*** and ***G***, Representative tracings of LV pressure and dP/dt_{max} and pressure-volume loops measured in NTG and HO-1 TG sham and HF hearts. *p < 0.05 vs. sham; #p < 0.05 vs. NTG HF. Sample size as noted in panel A.

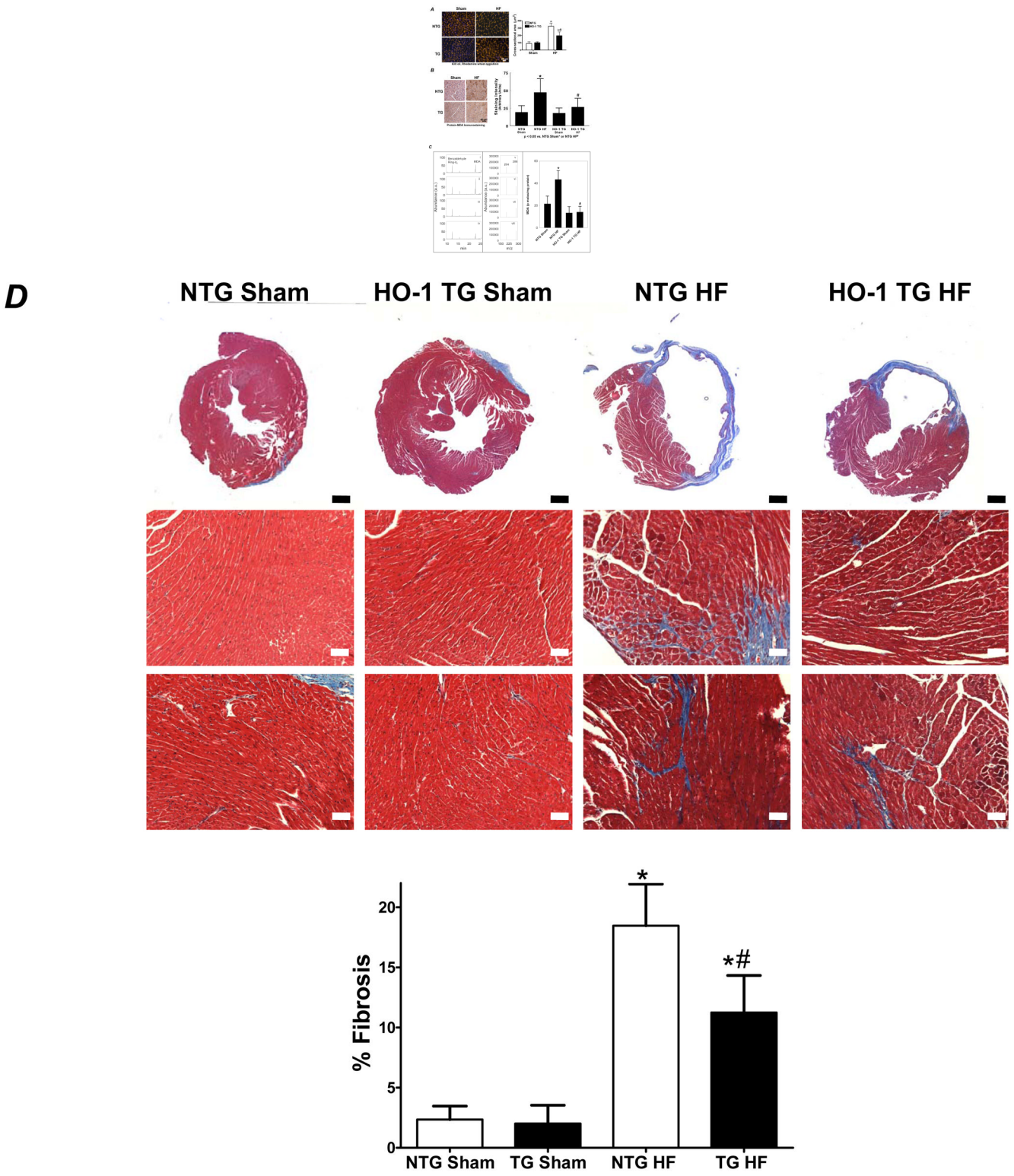

Figure 2.

Constitutive expression of HO-1 attenuates hypertrophy, fibrosis, and oxidative stress in HF. ***A***, Myocyte cell membrane staining with rhodamine wheat agglutinin. ***B***, Immunostaining

for MDA-adducted proteins in myocardium. ***C***, Myocardial free MDA levels by GC-NICI-MS. The left panel shows representative gas chromatograms of the MDA spectrum from NTG-sham (**i**), NTG-HF (**ii**), HO-1 TG sham (**iii**), and HO-1 HF (**iv**) hearts. The center panel shows typical spectra of ions with an m/z value of 204 (M^+-$C_7H_2F_5$-HFNO-C_2H_3) monitored for MDA quantitation in NTG-sham (**v**), NTG-HF (**vi**), HO-1 TG sham (**vii**), and HO-1 HF (**viii**) hearts. Benzaldehyde ring d_5 ion with m/z value of 286 (M^+-HF) was used as an internal standard. The right panel shows the quantitative group data. ***D***, Masson's trichrome staining in HO-1 TG and NTG sham and HF hearts. The black scale bar (2× magnification) is 1 mm and the white scale bar (10× magnification) is 125 μm. *$p < 0.05$ vs. sham; #$p < 0.05$ vs. NTG HF (n = 4–6/group).

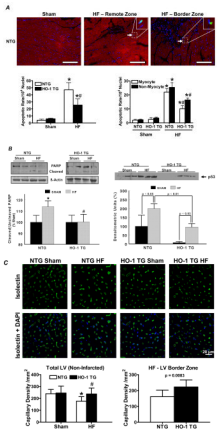

Figure 3.

HO-1 modulates apoptosis and neovascularization in the failing heart. ***A***, Representative TUNEL stains from a NTG sham and failing heart, and myocyte and non-myocyte apoptosis quantitation from NTG and HO-1 TG sham and heart failure (HF). Myocytes were identified by immunostaining with anti-troponin I antibody and Texas Red-conjugated secondary (red fluorescence), and nuclei were counterstained with DAPI (blue). TUNEL-positive nuclei appear green/cyan in the overlaid images. The scale bar is 225 μm. ***B***, Expression of cleaved and uncleaved PARP protein *and* the pro-apoptotic transcriptional activator p53 (Western blotting) in NTG and HO-1 TG sham and HF hearts. ***C***, Representative FITC-conjugated isolectin staining of myocardial capillaries (green fluorescence) and quantitation of capillary density from NTG and HO-1 TG sham and HF hearts. *$p < 0.05$ vs. sham; #$p < 0.05$ vs. NTG HF (n = 4–9/group).

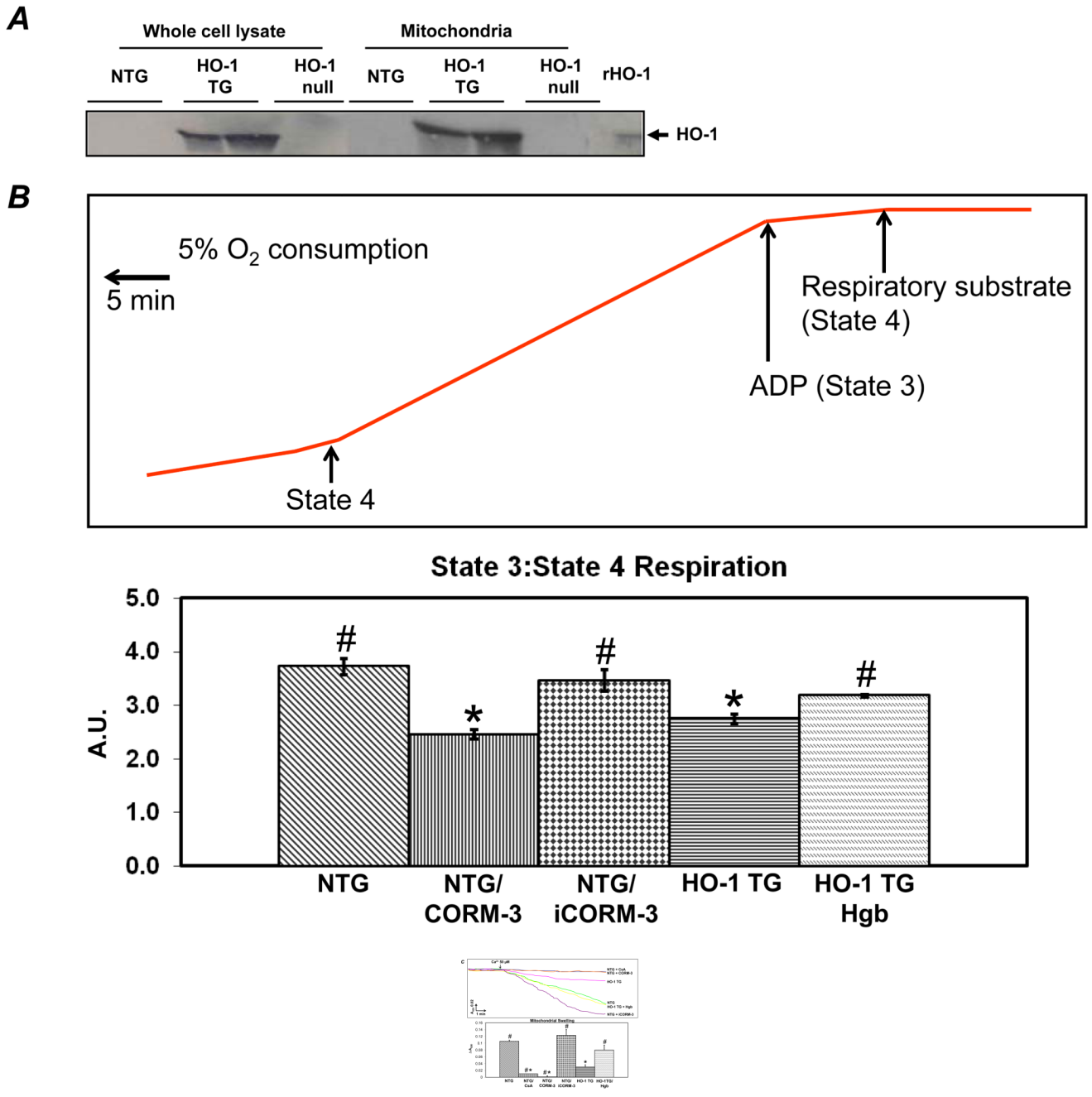

Figure 4.

HO-1 and CO suppress mitochondrial permeability transition (MPT) and respiration. ***A***, Western blots, developed using anti-HO-1 antibody, of whole cell cardiac lysates and mitochondrial fractions. ***B***, *Top*, Representative Clarke electrode recordings from isolated cardiac mitochondria. State 4 respiration was measured after the addition of Complex I respiratory substrates (10 mmol/L pyruvate and 5 mmol/L malate) and State 3 respiration following the addition of 0.33 mmol/L ADP. Oxygen consumption was calculated from the slope of tracing as indicated. *Bottom*, Group data for state 3:state 4 ratio in mitochondria isolated from NTG and HO-1-TG hearts with or without the indicated co-treatments (50 μmol/L CORM-3, iCORM, or hemoglobin [Hgb]). A.U., arbitrary units. ***C***, Ca^{2+}-induced

mitochondrial swelling (*i.e.*, decline in absorbance at 520 nm, A_{520}, an index of MPT) in cardiac mitochondria isolated from NTG or HO-1 TG hearts with or without the indicated pre-treatments: CORM-3, iCORM, hemoglobin (Hgb) (each at 50 μmol/L), cyclosporine A (CsA, 30 nmol/L, an inhibitor of MTP pore opening). Samples were pretreated 5 minutes before Ca^{2+} was added. *$p < 0.05$ vs. NTG, #$p < 0.05$ vs. HO-1 TG ($n = 4–7$ per group).

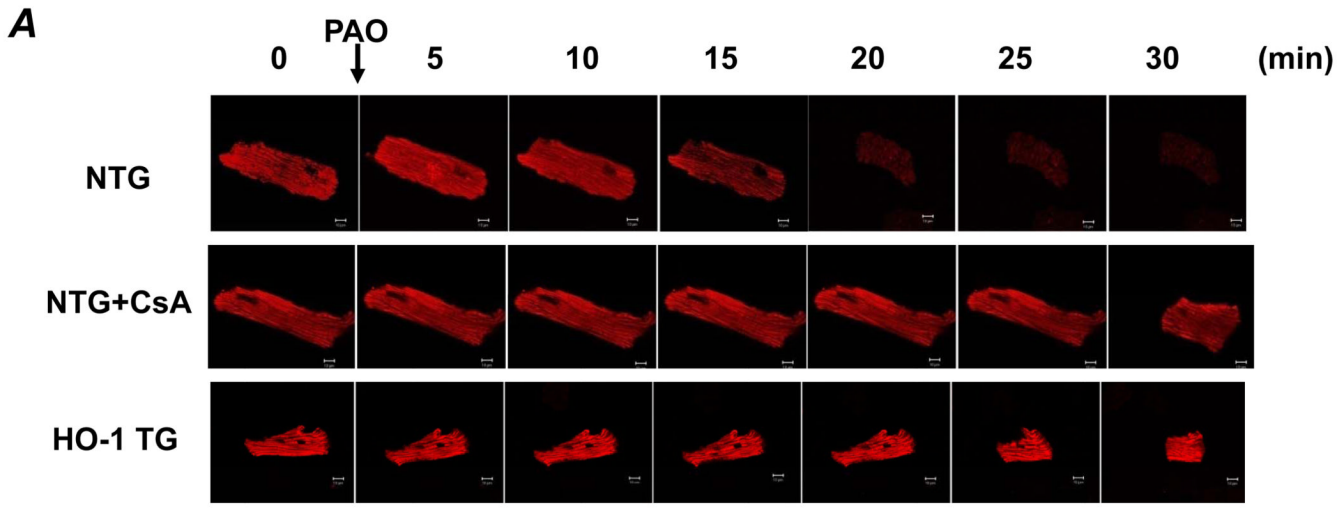

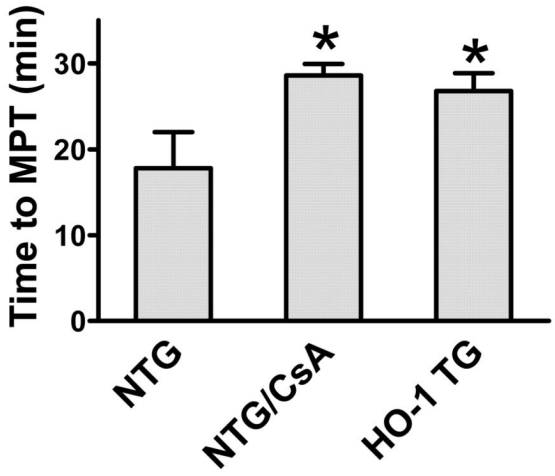

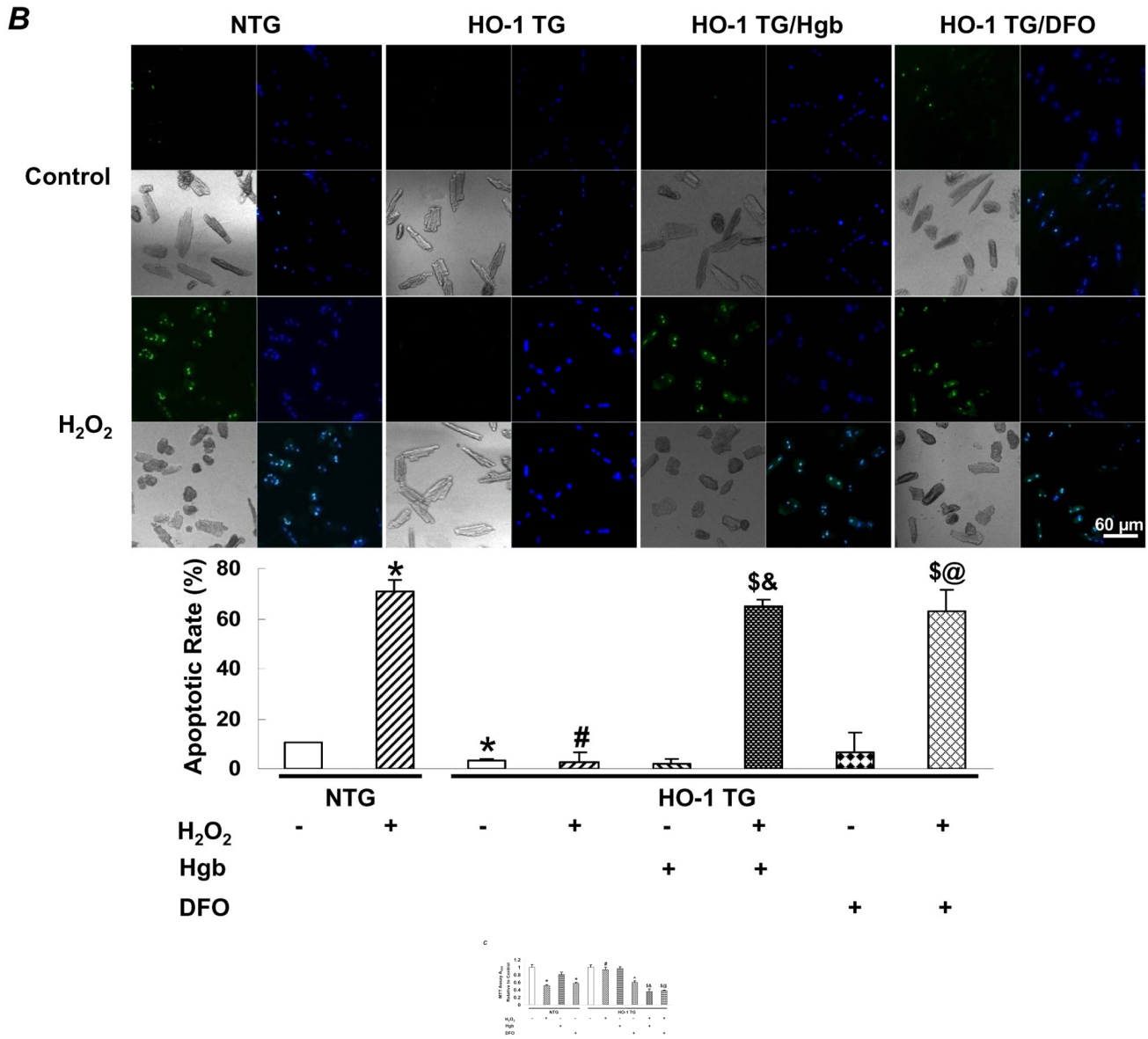

Figure 5.

HO-1 prevents MPT and apoptosis in cardiomyocytes in CO-dependent manner. ***A***, Mitochondrial membrane potential indexed by TMRM labeling (100 nmol/L for 30 min) in adult cardiomyocytes isolated from NTG or HO-1 TG hearts. Phenylarsine oxide (PAO, 20 μM) was used to induce MPT and CsA (100 nmol/L, introduced 5 min prior to PAO) was used to inhibit MPT. The time needed for a 2-fold decrease in TMRM fluorescence was used to quantify the development of MPT. *$p < 0.05$ vs. NTG; $n = 3–4$ per condition. The scale bar is 10 μm. ***B***, Adult NTG or HO-1 TG cardiomyocytes were exposed to 500 μM H_2O_2 for 1 h or media alone (control), with or without co-incubation with Hgb (50 μmol/L) or desferoxamine (DFO, 100 μmol/L) starting 30 min before H_2O_2. Shown for each condition (clockwise from top left) are representative confocal images of TUNEL staining (green fluorescence 520 nm), nuclear staining with DAPI (blue fluorescence 460 nm), overlaid images (TUNEL positive nuclei appear cyan), and phase contrast images. Quantitation of the apoptotic rate is shown in the graph. $p < 0.005$ versus: *NTG

control, #NTG H_2O_2, $HO-1 TG H_2O_2, &HO-1 TG Hgb, @HO-1 TG DFO; n = 3–4/group. ***C***, Overall cell survival measured by MTT assay under similar conditions as in ***B***. ^p < 0.005 vs. HO-1 TG control; n = 3–4/group.

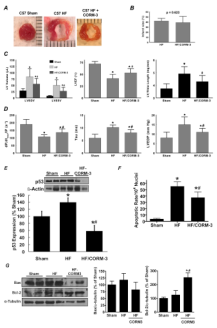

Figure 6.

CORM-3 treatment alleviates post-infarction LV remodeling. ***A***, representative LV sections from a sham mouse, a control heart failure (HF) mouse, and a HF mouse given CORM-3 40 mg/kg/day i.p. for 24 days starting 4 days after ligation. ***B***, Infarct size in untreated and CORM-3 treated HF. ***C***, Echocardiographic and gravimetric assessment of LV dilatation (LVEDV and LVESV), LV systolic function (LVEF), and LV hypertrophy (LV/tibia length). ***D***, Mechanical assessment of LV systolic function (dP/dt_{max}/IP) and diastolic performance (LVEDP and tau) in untreated and CORM-3 treated HF. ***E***, Western blotting for p53; ***F***, quantitation of apoptotic rate by TUNEL staining; and ***G***, Western blotting for Bax and Bcl-2 in sham, untreated HF, and CORM-3 treated HF hearts. *$p < 0.05$ vs. sham; #$p < 0.05$ vs. untreated HF ($n = 6–12$/group).

Table 1

LV Hemodynamics in NTG and HO-1 TG Sham and HF Mice

	NTG		HO-1 TG	
	Sham (n = 8)	HF (n = 11)	Sham (n = 7)	HF (n = 11)
HR	502 ± 30	463 ± 39*	500 ± 46	458 ± 25
LVEDV	25 ± 7	63 ± 15*	30 ± 9	41 ± 11*#
LVPSP	98 ± 17	87 ± 13	93 ± 11	90 ± 8
dP/dt_{max}	8248 ± 888	5301 ± 1169*	8230 ± 2107	6215 ± 777*#
dP/dt_{max}/IP	169 ± 56	103 ± 10*	159 ± 32	121 ± 15*#
dP/dt_{max}/EDV	361 ± 125	91 ± 40*	292 ± 81	166 ± 65*#
LVEDP	6 ± 5	14 ± 5*	6 ± 4	9 ± 4#
Tau	5.6 ± 2.1	9.2 ± 1.5*	6.4 ± 1.8	8.0 ± 1.0*#

LV, left ventricular; HR, heart rate (bpm); LVEDV, LV end-diastolic volume (μL); LVPSP, LV peak systolic pressure (mm Hg); dP/dt_{max}, maximal rate of change in LV pressure (mm Hg/s); dP/dt_{max}/IP, dP/dt_{max} normalized for instantaneous LV pressure (s^{-1}); dP/dt_{max}/EDV, dP/dt_{max} normalized for EDV (mm Hg/s•μL); LVEDP, LV end-diastolic pressure (mm Hg); tau, time constant of LV relaxation (ms); All values mean ± SD.

* $p < 0.05$ vs. respective sham,

# $p < 0.05$ vs. NTG HF.